

Adaptive Methods for Video Denoising Based on the ICI, FICI, and RICl Algorithms

Jonatan LERGA, Edi GRBAC, Victor SUCIC, Nicoletta SAULIG

Abstract: In various applications, reducing noise from video sequence is of crucial importance. In this paper, we have presented performance analysis of the novel video denoising method based on the relative intersection of confidence intervals (RICl) rule, and compared it to the methods based on the intersection of confidence intervals (ICI) rule and the fast ICI (FICI) rule. Detailed comparisons, based on two test video signals, are provided for a range of noise levels and different noise types. The RICl video denoising method has shown to outperform the original ICI based method, both in the algorithms execution time, reducing it by up to 11 %, and in the level of noise suppression, improving it by up to 10 dB. It also outperforms the FICI based video denoising method by up to 12.7 dB for the two test videos.

Keywords: intersection of confidence intervals (ICI) rule; locally adaptive filters; video denoising

1 INTRODUCTION

Real world video signals are often corrupted by various noise types during the acquisition and transmission processes [1÷4]. In order to extract the useful information from the noisy data, i.e., to reduce noise as much as possible, a powerful and robust denoising method is required. The main goal of such methods is to reduce noise levels so that the estimation error (for example, mean squared error (MSE)) is as small as possible, while desirable signal features, such as jumps or instantaneous slope changes, are well preserved [5]. As shown in [6], successful denoising techniques utilize locally adaptive, edge-sensitive algorithms which provide trade-off between the noise removal and the instantaneous slope changes and edges preserving.

This paper presents a novel video denoising method based on the relative intersection of confidence intervals (RICl) rule [4], which is compared to the methods based and the original intersection of confidence intervals (ICI) and the fast ICI (FICI) rule [8÷12]. The methods performance analysis is done on two real-life video signals.

The paper is organized as follows. Sections 2, 3 and 4 respectively outline the ICI, FICI, and RICl based methods with their characteristics and main features being described. Experimental results are presented and discussed in Section 5, while the conclusion is given in Section 6.

2 THE ICI METHOD

Let us consider a video pixel

$$y(i, j, k) = x(i, j, k) + v(i, j, k), \quad (1)$$

where $x(i, j, k)$ is the noise-free pixel and $v(i, j, k)$ is the noise in the considered pixel, while i and j are the pixel indices, and k stands for the video frame index.

Our goal is to find the best possible estimate $\hat{x}(i, j, k)$ from the noisy pixel $y(i, j, k)$, for each frame pixel of the video signal. In order to preserve useful features from the original noise-free pixel $x(i, j, k)$, i.e., to minimize the estimation error energy, a proper adaptive filter with adequate support selection is needed.

The ICI rule introduces a finite set of filter support sizes [11, 12]

$$D_n(i, j, k) = [L_n(i, j, k), U_n(i, j, k)], \quad (2)$$

and calculates the sequence of confidence intervals limits of the biased estimates for each video frame pixel independently to its left and right hand side. The confidence intervals are defined by their limits which are computed as [11, 12]

$$L_n(i, j, k) = \bar{x}_n(i, j, k) - z_c \frac{\sigma(i, j, k)}{\sqrt{n}}, \quad (3)$$

$$U_n(i, j, k) = \bar{x}_n(i, j, k) + z_c \frac{\sigma(i, j, k)}{\sqrt{n}}, \quad (4)$$

where $U_n(i, j, k)$ is the upper and $L_n(i, j, k)$ is the lower confidence interval limit, while $\bar{x}_n(i, j, k)$ represents the mean or median value of the considered video pixel(s) and $\sigma(i, j, k)$ estimation error standard deviation. Due to the \sqrt{n} term in the denominator of (3) and (4), each following confidence interval is narrower than the preceding one.

The ICI algorithm calculates the values of the smallest upper and the largest lower confidence intervals limits [11, 12], respectively as

$$\bar{L}_n(i, j, k) = \max_{n=1, \dots, N-k+1} (L_n(i, j, k)) \quad (5)$$

$$\underline{U}_n(i, j, k) = \min_{n=1, \dots, N-k+1} (U_n(i, j, k)). \quad (6)$$

Then, for each $n > 1$ it tracks the confidence intervals intersections with respect to the following condition [13, 14]

$$\bar{L}_n(i, j, k) \leq \underline{U}_n(i, j, k). \quad (7)$$

The largest n , for which (7) is satisfied, defines the proper filter support size that minimizes the estimation error [7, 9].

The confidence interval width and hence the confidence intervals intersection is controlled by the coefficient of confidence z_c [7, 9]. Too small values of z_c

provide narrow confidence intervals, i.e., they increase estimation variance and decrease estimation bias, resulting in undersized filter supports [7, 9]. On the other hand, too large z_c values give wider confidence intervals, i.e., they reduce estimation variance and increase estimation bias, resulting in oversized filter supports [7, 9]. Thus, the z_c value significantly affects the estimation performance. Selection procedure for a proper z_c value is explained in [2].

The absolute value of the estimation error can be calculated as

$$|e(i, j, k, h)| = |x(i, j, k) - \hat{x}(i, j, k, h)|, \quad (8)$$

where h is defined as filter support size. As shown in [9], the estimation error is

$$|e(i, j, k, h)| \leq |\omega(i, j, k, h)| + |\zeta(i, j, k, h)|, \quad (9)$$

where $\omega(i, j, k)$ is the estimation bias, and $\zeta(i, j, k)$ is a random error with the probability density $N(0, \sigma(i, j, k))$. Furthermore, as shown in [9], $|\zeta(i, j, k, h)| \leq \chi_{1-\alpha/2} \cdot \sigma(i, j, k, h)$ holds true with the probability $p = 1 - \alpha$, where $\chi_{1-\alpha/2}$ is the $(1-\alpha/2)^{\text{th}}$ quantile of the standard Gaussian distribution. Thus, the inequality (10) can be reduced (with the same probability) to

$$|e(i, j, k, h)| \leq |\omega(i, j, k, h)| + \chi_{1-\alpha/2} \cdot \sigma(i, j, k, h). \quad (10)$$

Once the filter support size is calculated using the ICI rule, the noise-free video estimates can be obtained by applying the mean filtering or median filtering to all pixel values in the calculated region. The above procedure is repeated for each pixel in the video signal, resulting in a noise-free video estimate.

3 THE FAST ICI (FICI) METHOD

In order to speed up the algorithm based on the ICI rule, a new faster approach is proposed, named the fast ICI (FICI) method. The method significantly reduces time needed for signal denoising, while maintaining acceptable quality level of the noise-free estimates.

The FICI method uses the modified algorithm for the filter support size selection and noise-free video estimate calculation. Unlike the original ICI based method, it does not calculate filter support sizes for each video pixel in each frame, but rather the filter support size for the first pixel in each detected time region, using the same filter support size for estimating all noise-free pixel values in the detected region.

The confidence intervals limits and their intersections for the FICI method are computed in the same way as in the ICI method, using Eqs. (3), (4) and (7). Due to the fact that the FICI based method calculates adaptive support filter size only for the first pixel in the detected region, the confidence intervals limits are computed only to the right hand side for each video pixel. On the other hand, the original ICI method requires both hand side calculations for each video pixel; hence ultimately resulting into longer denoising process.

Let us consider a video pixel in time, as the one in Eq. (1), with N being the number of video frames. The confidence intervals along with their intersections are tracked using the same procedure as in the ICI method, defined by (7). The first calculated filter support size, denoted as $h_1(i, j)$, is added to the filter support size set $\mathbf{H}(i, j)$ for the considered video pixel. If $h_1 \neq N$, the above procedure is repeated for $y(i, j, h_1 + 1)$, resulting in $h_2(i, j)$, also added to the $\mathbf{H}(i, j)$. The procedure is repeated until $\sum_{n=1}^{M(i, j)} h_n = N$ where $M(i, j)$ is the number of time regions for the considered pixel in time.

Thus, for the video pixel $y(i, j, k)$, the FICI method provides the filter support size set vector defined as

$$\mathbf{H}(i, j) = [h_1, \dots, h_n, \dots, h_{M(i, j)}], \sum_{n=1}^{M(i, j)} h_n = N, \quad (11)$$

and the time regions starting points set vector defined as

$$\mathbf{K}(i, j) = [k_1 = 1, k_2 = 1 + h_1, \dots, k_n = (1 + h_1 + \dots + h_{n-1})]. \quad (12)$$

Once all filter support sizes are calculated, the noise-free estimates can be obtained by applying either the mean filtering

$$\hat{x}_{mean}(i, j, k) = \frac{1}{h_n} \sum_{z=k_n}^{k_{n+1}-1} x(i, j, z), \quad k_n \leq k < k_{n+1}, \quad (13)$$

or the median filtering

$$\hat{x}_{median}(i, j, k) = \text{median}(x(i, j, k), \dots, x(i, j, k_{n+1}-1)), \quad k_n \leq k \leq k_{n+1}, \quad (14)$$

for each video pixel value in the detected region. The procedure is repeated for all video frame pixels.

4 THE RELATIVE ICI (RICl) METHOD

As shown in [7, 9], the proper value of the z_c parameter controls the quality of the signal estimate. Choosing the best z_c can be a long and numerically extensive task, sometimes even more challenging than the denoising itself. To overcome this limitation, a new method for the filter support selection, which does not require the knowledge of the optimal z_c parameter, has been proposed in [7].

Since the method tracks the amount of the overlapping of the confidence intervals intersection relative to the considered confidence interval length, it is named the relative ICI (RICl) method. The method improves the original ICI based method by introducing an additional criterion for the filter support size selection, defined as the ratio of the confidence interval intersection and the considered confidence interval size

$$R_n(i, j, k) = \frac{U_n(i, j, k) - \bar{L}_n(i, j, k)}{U_n(i, j, k) - L_n(i, j, k)} = \frac{U_n(i, j, k) - \bar{L}_n(i, j, k)}{2z_c \frac{\sigma(i, j, k)}{\sqrt{n}}}. \quad (15)$$

Unlike the original ICI based method, the RICl based method calculates the filter support size as the largest one satisfying the following condition [7]

$$R_n(i, j, k) \geq R_c, \quad (16)$$

where R_c is the preset threshold value. The threshold R_c can be chosen using the formula proposed in [5]

$$R_c = 0.0069z_c^3 - 0.1141z_c^2 + 0.6748z_c - 0.4867, \quad 2.5 \geq z_c \leq 5. \quad (17)$$

As described in [5], R_c belongs to the finite interval $[0,1]$, hence making its selection much easier task than finding a proper z_c value. For $R_c = 0$, the RICl method becomes the original ICI method, while for all $0 < R_c \leq 1$ values, the RICl rule was shown to significantly outperform the original ICI rule [7] when used in signal denoising.

The RICl rule in [7] was applied to 1D signals only. In this paper, the method is extended in a way to be applicable to video denoising as well. As shown in Section 5, the RICl based method significantly outperforms the original ICI and FICI based methods. For the test video signals used in this paper, the z_c value was set to 4.4 (as in [9]), and the R_c value was found to be 0.86, by using equation (17). The comparison of the results obtained using the mean and median filtering for various noise levels and noise types (additive white Gaussian noise and impulsive Poisson noise) for the three presented methods is given in the next section.

5 DENOISING RESULTS

The performances of the here described video denoising algorithms are analyzed and compared for the two real-life test video signals obtained by recording a moving object passing through a stationary scene. The detailed comparison between the methods is given for a range of noise levels, as well as for different noise types, in terms of the average peak signal-to-noise ratio (PSNR) improvement, used as a measure of video estimation quality. The comparison with the fixed filter support size based methods is given in [15, 16].

The first test video is composed of 149 video frames, recorded using the 25 frames per second rate, with resolution of 320×248 pixels. The noise-free video frame, along with a noisy frame corrupted by the additive white Gaussian noise (AWGN) and the impulsive Poisson noise, are given in Figs. 1(a), 1(b) and 1(c), respectively. Figs. 1(d) and 1(e) show the denoised video frame for the AWGN, while Figs. 1(f) and 1(g) show the denoised video frame for the Poisson noise, both obtained using the ICI rule based method after applying mean and median filtering, respectively. Video frames obtained using the FICI based method are given in Figs. 1(h)-1(k), while the results obtained using the RICl based method are shown in Figs. 1(l)-1(o). As it can be seen from Figs. 1(l)-1(o), denoising based on the RICl rule has significantly suppressed the noise present in the noisy video, the moving object has not been blurred, and its edges are well preserved. The average frame PSNR was improved by up to 12.69 dB (see Tab. 1). When compared to the results

obtained using the ICI method, as shown in Figs. 1(d)-1(g), the RICl method significantly outperformed the original ICI method by up to 10.07 dB.

Table 1 gives the denoising results using the here described methods for the first test video, for various noise levels, as well as different noise types. The type of filtering (mean and median), used for calculating the noise free estimate once the filter support size is detected, has negligible effect on the achieved PSNR and no visual difference is noticed in the denoised figures.

The first column of Tab. 1 gives the average frame PSNR values for the noisy video; while the second and the third column present the PSNRs for the video denoised using the ICI based method for mean and median filtering (AWGN), respectively. The fourth and the fifth column present PSNRs obtained using the ICI based method for mean and median filtering (for Poisson noise), respectively. Results for video denoised using the FICI based method are shown in columns 6-9, while the results achieved using the RICl based method are given in columns 10-13. The RICl method has increased the average frame PSNR by up to 10.36 dB when compared to the noisy video signal, while the original ICI method has increased the average frame PSNR by up to 3.46 dB, as shown in Tab. 1.

The FICI method, unlike the original ICI and RICl rule based methods, has additionally corrupted the noisy video frame, as shown in Figs. 1(h)-1(k) and Tab. 1. However, the total execution time for denoising the whole video signal using the FICI based method was significantly reduced (by up to 98% when compared to the original ICI method). Also, it managed to clear the noise from the stationary scene background.

The second test video is composed of 150 video frames, recorded using the 29 frames per second rate, with resolution of 300×180 pixels. The noise-free video frame, along with a noisy frame corrupted by the AWGN and impulsive Poisson noise, are given in Figs. 2(a), 2(b) and 2(c), respectively. Figs. 2(d) and 2(e) give the denoised video frame for the AWGN, while Figs. 2(f) and 2(g) give the denoised video frame for the Poisson noise, both obtained using the ICI method after applying mean and median filtering, respectively. The results obtained using the FICI based method are shown in Figs. 2(h)-2(k), while the results obtained by the RICl based method are shown in Figs. 2(l)-2(o).

The RICl based method has preserved the moving object edges without blurring it, as it can be seen in Figs. 2(l)-2(o). The average frame PSNR was improved by 8.9 dB when compared to the original ICI based method, as given in Tab. 2, hence yielding significant noise suppression.

The FICI rule based method has significantly reduced the algorithms execution time, as shown in Tab. 3, when compared to the original ICI and RICl method. However, the FICI based method resulted in poor denoising and blurring of the moving object in the video. On the other hand, the RICl based method has increased the average PSNRs by up to 10.17 dB when compared to the noisy video signal, unlike the ICI based method which has increased PSNRs by up to 4.21 dB.

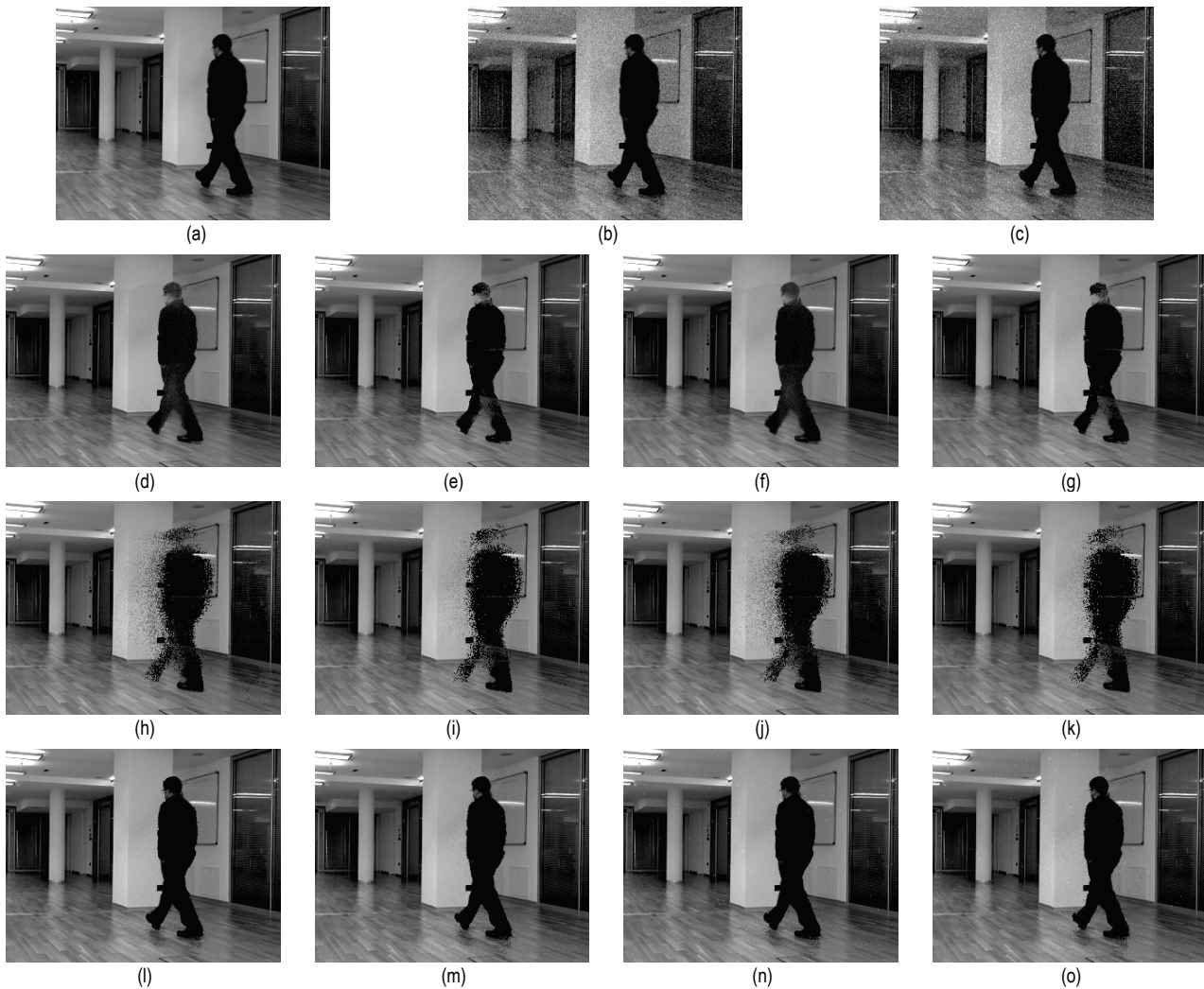


Figure 1 First test video. (a) Original noise-free video frame. (b) Noisy frame corrupted by the AWGN. (c) Noisy frame corrupted by the impulse Poisson noise. (d) Denoised frame using the ICI based method with mean filtering for the AWGN. (e) Denoised frame using the ICI based method with median filtering for the AWGN. (f) Denoised frame using the ICI based method with mean filtering for the impulse Poisson noise. (g) Denoised frame using the ICI based method with median filtering for the impulse Poisson noise. (h) Denoised frame using the FICI based method with mean filtering for the AWGN. (i) Denoised frame using the FICI based method with median filtering for the AWGN. (j) Denoised frame using the FICI based method with mean filtering for the impulse Poisson noise. (k) Denoised frame using the FICI based method with median filtering for the impulse Poisson noise. (l) Denoised frame using the RICl based method with mean filtering for the AWGN. (m) Denoised frame using the RICl based method with median filtering for the AWGN. (n) Denoised frame using the RICl based method with mean filtering for the impulse Poisson noise. (o) Denoised frame using the RICl based method with median filtering for the impulse Poisson noise.

Table 1 Average frame PSNR values for the first test video, denoised using the three methods for a range of noise levels and different noise types

Average frame PSNR												
Noisy video	ICI				FICI				RICl			
	Gaussian		Poisson		Gaussian		Poisson		Gaussian		Poisson	
	Mean	Med	Mean	Med	Mean	Med	Mean	Med	Mean	Med	Mean	Med
42.15	39.50	39.37	39.53	39.24	37.98	37.76	38.00	37.79	45.63	45.29	45.46	44.78
34.14	33.87	35.09	33.90	34.96	28.97	28.54	28.97	28.61	40.20	39.78	39.97	38.91
28.09	28.45	31.34	28.48	31.27	23.84	23.30	23.81	23.23	36.35	35.91	36.12	35.18
24.59	25.03	27.44	25.08	27.31	21.48	20.85	21.48	20.69	33.97	33.54	33.50	32.58
22.12	22.72	23.45	22.75	23.28	20.10	19.67	19.92	19.51	32.08	31.66	31.50	30.74
18.61	19.73	18.59	19.78	18.56	18.20	17.45	18.21	17.54	28.97	28.66	28.30	27.48
14.15	17.55	17.09	17.61	17.12	17.71	17.15	17.74	17.20	23.67	23.19	23.06	22.71

Tab. 3 gives the execution time of all three here described denoising algorithms for complete video denoising, both for the mean and median filtering and for both AWGN and impulsive Poisson noise. We have used Toshiba A660 notebook powered by Intel® Core™ i5 CPU M 430 @ 2.27 GHz with 4 GB of RAM. The FICI based method was shown to reduce the algorithm

execution time by up to 98 % when compared to the original ICI based method, but resulting into poorer denoising results.

On the other hand, the RICl method has outperformed the original ICI based method both in the algorithm execution time (reducing it by up to 11 %) and noise suppression (increasing PSNR by up to 10.07 dB).

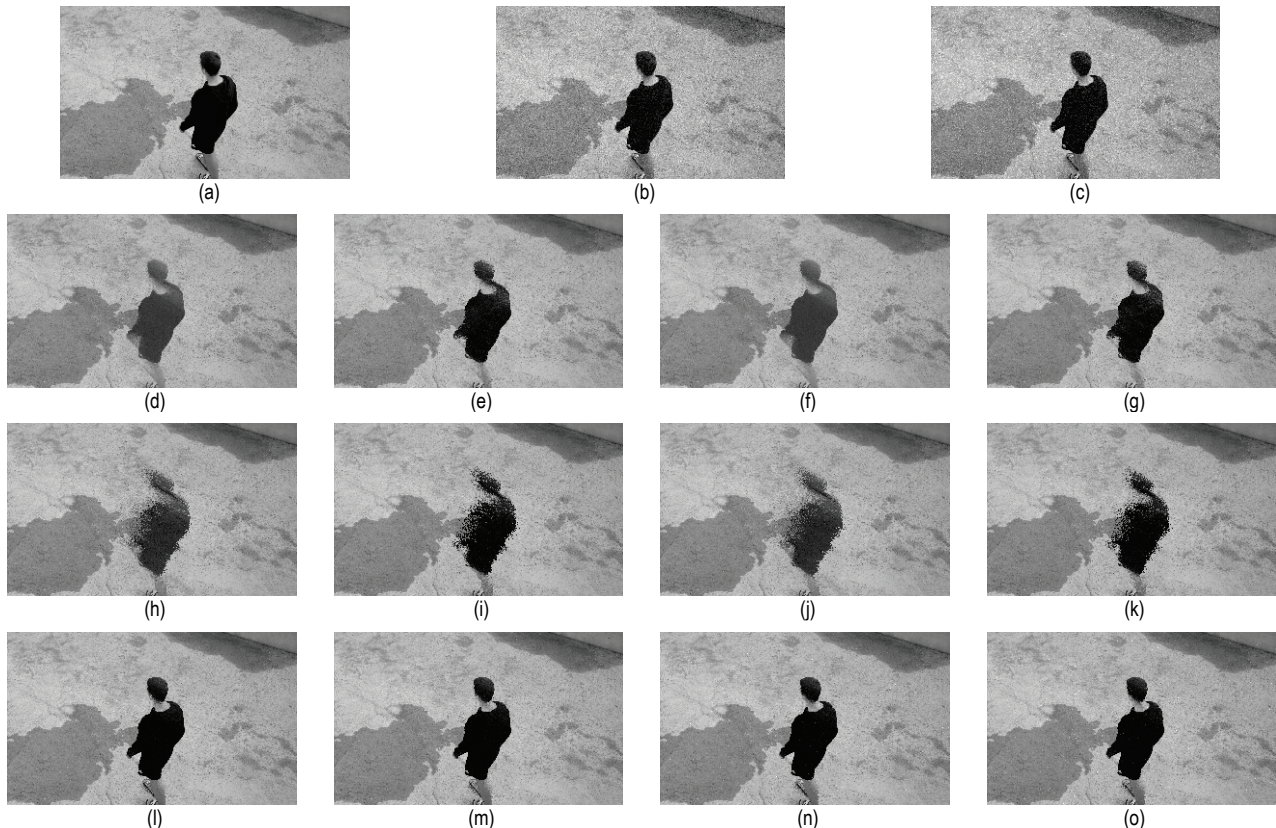


Figure 2 Second test video. (a) Original noise-free video frame. (b) Noisy frame corrupted by the AWGN. (c) Noisy frame corrupted by the impulse Poisson noise. (d) Denoised frame using the ICI based method with mean filtering for the AWGN. (e) Denoised frame using the ICI based method with median filtering for the AWGN. (f) Denoised frame using the ICI based method with mean filtering for the impulse Poisson noise. (g) Denoised frame using the ICI based method with median filtering for the impulse Poisson noise. (h) Denoised frame using the FICI based method with mean filtering for the AWGN. (i) Denoised frame using the FICI based method with median filtering for the AWGN. (j) Denoised frame using the FICI based method with mean filtering for the impulse Poisson noise. (k) Denoised frame using the FICI based method with median filtering for the impulse Poisson noise. (l) Denoised frame using the RICl based method with mean filtering for the AWGN. (m) Denoised frame using the RICl based method with median filtering for the AWGN. (n) Denoised frame using the RICl based method with mean filtering for the impulse Poisson noise. (o) Denoised frame using the RICl based method with median filtering for the impulse Poisson noise.

Table 2 Average frame PSNR values for the second test video, denoised using the three methods for a range of noise levels and different noise types

Average frame PSNR for second video												
Noisy video	ICI				FICI				RICl			
	Gaussian		Poisson		Gaussian		Poisson		Gaussian		Poisson	
	Mean	Med	Mean	Med	Mean	Med	Mean	Med	Mean	Med	Mean	Med
42.15	38.93	38.83	38.96	38.85	37.00	36.71	36.83	36.58	43.26	42.82	43.10	42.63
34.14	34.27	34.86	34.31	34.85	29.53	29.15	29.61	29.30	38.91	38.60	38.62	37.95
28.09	28.59	31.08	28.58	31.07	24.68	24.01	24.58	23.95	35.91	35.42	35.45	34.38
24.59	25.37	27.56	25.43	27.28	22.60	21.85	22.60	21.84	33.87	33.47	33.12	32.31
22.12	23.25	24.35	23.28	24.21	21.05	20.43	20.94	20.29	32.15	31.67	31.44	30.71
18.61	20.48	19.96	20.53	19.83	19.29	18.76	19.26	18.61	28.78	28.61	28.14	27.80
14.15	18.29	17.88	18.36	18.06	18.40	17.95	18.47	18.03	24.15	23.86	23.74	22.91

Table 3 Execution time for the three algorithms

Algorithm execution time (in minutes)												
Video	ICI				FICI				RICl			
	Gaussian		Poisson		Gaussian		Poisson		Gaussian		Poisson	
	Mean	Med	Mean	Med	Mean	Med	Mean	Med	Mean	Med	Mean	Med
First	186.21	167.27	167.98	169.09	3.91	4.29	4.02	4.03	165.55	169.51	162.35	163.65
Second	127.2	113.90	111.01	111.13	2.47	2.48	2.70	2.78	113.81	112.13	112.29	111.49

6 CONCLUSION

In this paper, a signal denoising method based on the relative intersection of confidence intervals (RICl) rule has been applied to video denoising. The method's performance was analyzed and compared to the results obtained using the original intersection of confidence intervals (ICI) and fast ICI based methods.

The RICl based video denoising method was shown to outperform the original ICI based method in algorithms execution time reduction, as well as in noise suppression, for the two test videos and different noise levels and noise types. The method was shown to increase denoised video average frame PSNRs by up to 10.7 dB when compared to the original ICI based method, and by up to 10.36 dB when compared to the noisy videos. Furthermore, the RICl based method has increased the algorithm speed by

up to 11 % when compared to the original ICI based method.

Therefore, the RICl based method was shown to be efficient not only for 1D signals and image denoising, but, as confirmed by the here presented results, in video denoising too. It has outperformed the original ICI based method both in terms of the estimation quality improvement and the algorithm execution time reduction.

7 REFERENCES

- [1] Romić, K., Galić, I., & Baumgartner, A. (2012). Character Recognition based on Region Pixel Concentration for License Plate Identification. *Technical Gazette*, 19(2), 321-325.
- [2] Singh, C. & Aggarwal, A. (2017). An Efficient Approach for Image Sequence Denoising Using Zernike Moments-Based Nonlocal Means Approach. *Computers & Electrical Engineering*, 62(C), 330-344.
<https://doi.org/10.1016/j.compeleceng.2015.09.006>
- [3] Hadj Fredj, A. & Malek, J. (2017). GPU-Based Anisotropic Diffusion Algorithm for Video Image Denoising. *Microprocessors and Microsystems*, 53(C), 190-201.
<https://doi.org/10.1016/j.micpro.2017.08.003>
- [4] Priego, B., Duro, R. J., & Chanussot, J. (2017). 4DCAF: A Temporal Approach for Denoising Hyperspectral Image Sequences. *Pattern Recognition*, 72, 433-445.
<https://doi.org/10.1016/j.patcog.2017.07.023>
- [5] Sucić, V., Lerga, J., & Vrankić, M. (2013). Adaptive Filter Support Selection for Signal Denoising based on the Improved ICI Rule. *Digital Signal Processing*, 23(1), 65-74. <https://doi.org/10.1016/j.dsp.2012.06.014>
- [6] Stanković, Lj. (2001). Performance Analysis of the Adaptive Algorithm for Bias-to-Variance Tradeoff. *IEEE Trans. Signal Process.*, 52(5), 1228-1234.
<https://doi.org/10.1109/TSP.2004.826179>
- [7] Lerga, J., Vrankić, M., & Sucić, V. (2008). A Signal Denoising Method Based on the Improved ICI Rule. *IEEE Signal Processing Letters*, 15, 601-602.
<https://doi.org/10.1109/LSP.2008.2001817>
- [8] Goldenshluger, A. & Nemirovski A. (1997). On Spatial Adaptive Estimation of Nonparametric Regression. *Mathematical Methods of Statistics*, 6, 135-170.
- [9] Katkovnik, V. (1999). A New Method for Varying Adaptive Bandwidth Selection. *IEEE Transactions on Signal Processing*, 47(9), 2567-2571.
<https://doi.org/10.1109/78.782208>
- [10] Katkovnik, V. & Shmulevich, I. (2002). Kernel Density Estimation with Adaptive Varying Window Size. *Pattern Recognition Letters*, 23, 1641-1648.
[https://doi.org/10.1016/S0167-8655\(02\)00127-7](https://doi.org/10.1016/S0167-8655(02)00127-7)
- [11] Lerga, J., Grbac E., & Sucić, V. (2014). An ICI Based Algorithm for Fast Denoising of Video Signals. *Automatika*, 55(3), 351-358.
<https://doi.org/10.7305/automatika.2014.12.525>
- [12] Seršić, D. & Sović, A. (2013). A robust separable image denoising based on relative intersection of confidence intervals rule. *ISPA 2013*, 89-96.
- [13] Egiazarian K., Katkovnik, V., & Astola, J. (2001). Adaptive Window Size Image Denoising Based on ICI Rule. *Acoustics, Speech, and Signal Processing (ICASSP '01), Proc. of the 2001 IEEE International Conference on*, 3, 1869-1872.
<https://doi.org/10.1109/ICASSP.2001.941308>
- [14] Katkovnik V., Egiazarian, K., & Astola, J. Adaptive Varying Scale Methods in Image Processing - Part I: Denoising and Deblurring, Tampere, Finland, 2003.
- [15] Grbac, E., Lerga, J., & Sucić, V. (2011). Video Denoising Using The ICI Method. *Innovative Technologies (IN-TECH 2011), Proc. of 2011 International Conference on*, Bratislava, Slovakia, 182-186.
- [16] Lerga, J., Sucić, V., & Grbac, E. (2012). An Adaptive Method for Video Denoising Based on the ICI Rule. *Engineering Review*, 32(1), 33-40.

Contact information:

Doc. dr. sc. **Jonatan LERGA**

Corresponding author
Faculty of Engineering, University of Rijeka
Vukovarska 58, HR-51000 Rijeka, Croatia
jlerga@riteh.hr

Edi GRBAC, B.Sc.

Faculty of Engineering, University of Rijeka
Vukovarska 58, HR-51000 Rijeka, Croatia
egrbac@riteh.hr

Prof. dr. sc. **Victor SUCIĆ**

Faculty of Engineering, University of Rijeka
Vukovarska 58, HR-51000 Rijeka, Croatia
vsucic@riteh.hr

Doc. dr. sc. **Nicoletta SAULIG**

Department of Engineering, Juraj Dobrila University of Pula
Zagrebačka 30, HR-52100 Pula, Croatia
nsaulig@unipu.hr